Journal of Biomedical Optics

SPIEDigitalLibrary.org/jbo

Single-virus tracking approach to reveal the interaction of Dengue virus with autophagy during the early stage of infection

Li-Wei Chu
Yi-Lung Huang
Jin-Hui Lee
Long-Ying Huang
Wei-Jun Chen
Ya-Hsuan Lin
Jyun-Yu Chen
Rui Xiang
Chau-Hwang Lee
Yueh-Hsin Ping

Single-virus tracking approach to reveal the interaction of Dengue virus with autophagy during the early stage of infection

Li-Wei Chu,[a,c] Yi-Lung Huang,[a,c] Jin-Hui Lee,[a,c] Long-Ying Huang,[b] Wei-Jun Chen,[a,c] Ya-Hsuan Lin,[a,c] Jyun-Yu Chen,[a,c] Rui Xiang,[a,c] Chau-Hwang Lee,[a,c,f] and Yueh-Hsin Ping[a,b,c,d,e]
[a]National Yang-Ming University, Institute of Biophotonics, Taipei, Taiwan
[b]National Yang-Ming University, Department and Institute of Pharmacology, Taipei, Taiwan
[c]National Yang-Ming University, Biophotonics and Molecular Imaging Research Center, Taipei, Taiwan
[d]National Yang-Ming University, Infection and Immunity Research Center, Taipei, Taiwan
[e]National Yang-Ming University, Cancer Research Center & VYM Genome Research Center, Taipei, Taiwan
[f]Academia Sinica, Research Center for Applied Sciences, Taipei, Taiwan

Abstract. Dengue virus (DENV) is one of the major infectious pathogens worldwide. DENV infection is a highly dynamic process. Currently, no antiviral drug is available for treating DENV-induced diseases since little is known regarding how the virus interacts with host cells during infection. Advanced molecular imaging technologies are powerful tools to understand the dynamics of intracellular interactions and molecular trafficking. This study exploited a single-virus particle tracking technology to address whether DENV interacts with autophagy machinery during the early stage of infection. Using confocal microscopy and three-dimensional image analysis, we showed that DENV triggered the formation of green fluorescence protein-fused microtubule-associated protein 1A/1B-light chain 3 (GFP-LC3) puncta, and DENV-induced autophagosomes engulfed DENV particles within 15-min postinfection. Moreover, single-virus particle tracking revealed that both DENV particles and autophagosomes traveled together during the viral infection. Finally, in the presence of autophagy suppressor 3-methyladenine, the replication of DENV was inhibited and the location of DENV particles spread in cytoplasma. In contrast, the numbers of newly synthesized DENV were elevated and the co-localization of DENV particles and autophagosomes was detected while the cells were treated with autophagy inducer rapamycin. Taken together, we propose that DENV particles interact with autophagosomes at the early stage of viral infection, which promotes the replication of DENV.
 [DOI: 10.1117/1.JBO.19.1.011018]

Keywords: Dengue virus; autophagy; autophagosome; single-virus particle tracking.

Paper 130286SSRR received Apr. 26, 2013; revised manuscript received Sep. 30, 2013; accepted for publication Oct. 9, 2013; published online Nov. 5, 2013.

1 Introduction

Dengue virus (DENV) infection is an emerging epidemic infectious disease with more than 50 million cases of infection, leading to an approximately 5% mortality rate annually, across approximately 100 countries with potential for further spread.[1,2] DENV infection causes a wide spectrum of clinical symptoms, ranging from asymptomatic infection or self-limited febrile illness named Dengue fever (DF) to life-threatening diseases including Dengue hemorrhagic fever and Dengue shock syndrome.[3,4] Unfortunately, neither antiviral drugs nor vaccines to treat or prevent DENV infection are currently available. There remains an incomplete understanding on the mechanism underlying the process of virus infection as well as pathogenesis, which limits the development of antiviral agents. Little is known about the pathogenesis of severe DENV-induced illnesses, although the magnitude of DENV replication is considered as one of the major critical factors.[5]

DENV is highly dependent on its host cell for the replication. Not only does the host cell supply essential elements for viral metabolism, but it also provides a structural platform for the replication of the viral genome and the assembly of viral particles. Viral infection begins with the attachment of virus particles to the host cellular membrane, in which viral E protein interacts with cellular receptors present on the surface of host cells.[6] Following internalization, DENV particles are transported to Rab5-positive endosomes, which subsequently mature into late endosomes through acquisition of Rab7 and loss of Rab5.[7,8] Fusion of the viral membrane with the endosomal membrane is primarily detected in late endosomal compartments.[8–10] The DENV core protein is then released into the host cytoplasm and translocated into the nucleus to perturb host gene expression.[11] The RNA genome is translated to produce viral proteins followed by transcription and replication of RNA close to the endoplasmic reticulum (ER).[12] The entire process is dependent on the movement of the virus particles and viral components within the host cells. Although the major events of the DENV infection process are broadly understood, details regarding entry and intracellular trafficking of DENV have not been revealed comprehensively.

Autophagy essential for survival, development, and homeostasis is a highly conserved catabolic process for the degradation of cellular materials including damaged or excess organelles and

Address all correspondence to: Yueh-Hsin Ping, National Yang-Ming University, Department and Institute of Pharmacology, Shih-Pai, Taipei 112, Taiwan. Tel: +886-2-2826-7326; Fax: +886-2-28264372; E-mail: yhping@ym.edu.tw

0091-3286/2014/$25.00 © 2014 SPIE

protein aggregates through a lysosomal degradation pathway. Autophagy begins with the formation of the isolated membrane and then continues to stretch and mature into a double-membrane vesicle named an autophagosome with a diameter ranging from 500 to 1000 nm (see recent comprehensive reviews[13,14]). Autophagosomes fuse with endosomes to generate amphisomes that subsequently fuse with lysosomes to form autophagolysosomes.[14] Autophagy can work either in a nonselective mode induced by starvation for supplying energy to cells or in a highly selective mode involving the recruitment of specific adaptor proteins that recognize particular targeted organelles or vesicles to form autophagosomes.[14] In addition to regular cellular metabolism, autophagy also participates in a wide spectrum of disease progressions including viral infection.[15,16] Growing evidence showed that infections with various DNA or RNA viruses stimulate an increasing amount of autophagic vesicles such as autophagosomes in infected cells, suggesting that autophagy is activated upon virus infection.[16–20] Several independent studies have shown that DENV infection is able to induce autophagy, and autophagy is required for the RNA genome replication of DENV.[21–25] In addition, DENV-induced autophagy was found to regulate cellular lipid metabolism required for the efficient DENV replication.[21] Taken together, these studies supported that autophagy is a critical cellular factor involved in DENV replication. However, the interaction between DENV and the components of autophagy and the timing of the interaction during the infection are poorly understood.

Visualizing and quantifying molecular interactions are important issues in biomedical studies. Virus infections are complicated processes, which include multistep transports, dynamic interactions with various cellular factors, and dynamic changes within the cellular structures. Moreover, there are various routes and intracellular transports for the same virus in host cells. Following the fate of individual virus particles using a single-virus particle tracking technology allows us to probe dynamic interactions between virus and cellular factors and to dissect the steps of the infectious process.[26] Using epi-fluorescence microscopy, single-virus tracking can monitor individual virus particles or viral components in living cells.[27–33] Tracking a single genetic particle in a living cell provides direct evidence to identify interactions between the particle and the specific cellular machinery. In particular, the physical trajectory of a single viral particle is capable of offering unambiguous insights into its transport mechanisms.[28,34,35] In the present study, combining biophotonics and conventional virology approaches, we elucidated that DENV could trigger autophagy at the early stage of infection and DENV particles traveled into autophagosomes 30 min after clathrin-mediated endocytosis resulting in the promotion of viral replication.

2 Materials and Methods

2.1 *Cell Cultures*

Microtubule-associated protein 1A/1B-light chain 3 (LC3) is the reputable marker of autophagosomes in mammalian cells.[36] Stably expressed green fluorescence protein-fused microtubule-associated protein 1A/1B-light chain 3 (GFP-LC3) Huh7.5 cell line produced by transduction of cells with lentiviruses expressing GFP-LC3 was generously provided by Dr. Michael M.C. Lai (Institute of Molecular Biology, Academia Sinica, Taipei, Taiwan).[37] GFP-LC3 Huh7.5 cells were maintained in high-glucose Dulbecco's modified Eagle's medium (DMEM, GIBCO, USA) supplemented with 10% fetal bovine serum (FBS) (HyClone, Thermo, USA), 1% nonessential amino acids (NEAA, GIBCO, USA), 4 μg/ml blasticidin (Invitrogen, USA). The cells were cultivated at 37°C in a humidified atmosphere with 5% CO_2. The *Aedes albopictus* C6/36 cell line, useful for propagation of flaviviruses, was cultured in RPMI 1640 medium (GIBCO, USA) supplemented with 10% FBS, 1% NEAA, 2% penicillin/streptomycin (GIBCO, USA), and 1 mM sodium pyruvate (Biological Industries, Kibbutz Beit-Haemek, Israel) and cultivated at 28°C in a humidified atmosphere with 5% CO_2. The baby hamster kidney cell line BHK-21 was maintained in high-glucose DMEM supplemented with 10% FBS and 2% penicillin/streptomycin at 37°C and 5% CO_2.

2.2 *DENV Propagation and Infection*

DENV serotype 2 strain 16681 was propagated in confluent monolayers of C6/36 cells. Cells were inoculated with virus supernatant and incubated for 90 min at 28°C with gentle rocking at 15-min intervals for virus adsorption. Afterward, maintenance medium (RPMI 1640 with 5% FBS) was added and incubated at 28°C for 5 to 7 days. Infected cell culture medium was collected; cell debris was removed by centrifugation, and virus supernatant was aliquoted and stored. For virus infection, Huh7.5 cells were adsorbed with DENV at a multiplicity of infection (MOI) of 10 at 4°C for 30 min to synchronize viral entrance. The cells were then washed once with PBS to remove unbound viral particles and incubation temperature was switched to 37°C. To repress or stimulate cellular autophagic response, GFP-LC3 Huh7.5 cells were either pretreated with 10 mM of 3-methyladenine (3-MA; Sigma–Aldrich, USA) or with 100 nM of rapamycin (Sigma–Aldrich, USA) in serum free DMEM at 4°C for 30 min prior to DENV infection.

2.3 *Plaque Quantitation Assay*

A sample vial of virus suspension to be quantified was diluted in 10-fold step with serum-free DMEM. BHK-21 was seeded in 6-well plates (4×10^5 cells/well) and incubated overnight at 37°C. The medium was then aspirated and 100 μl of serially diluted viral suspension were added. After 2-h incubation at 37°C with gentle rocking at 15-min intervals, the cells were overlaid DMEM containing 1% low-melting agarose (Lonza, Switzerland) and 2% heat-inactivated FBS. Six-days postinfection, the overlaid medium was then removed, and cells were fixed with 10% formaldehyde (Sigma–Aldrich, USA) and stained with the 1% crystal violet (Sigma–Aldrich, USA). The end-point titer was determined by macroscopic counting of plaques.

2.4 *Preparation of Fluorescence-Labeled DENV Particles*

DENV particles were labeled with the lipophilic fluorescent dye DiD (1,1′-dioctadecyl-3,3,3′,3′-tetramethylindodicarbocyanine, 4-chlorobenzenesulfonate salt) (Invitrogen, USA), with the maximum absorption at 630 nm and the maximum emission at 670 nm, as described previously with the minor modification.[8,28,38] Briefly, 1×10^7 pfu/ml of DENV was mixed with 2 nmol of DiD dissolved in dimethyl sulfoxide in HNE buffer [5 mM 2-[4-(2-hydroxyethyl)piperazin-1-yl]ethanesulfonic acid (HEPES), 150 mM NaCl, 0.1 mM ethylenediamine tetra-acetic acid, pH 7.4] for 10 min. The unincorporated dye was separated

from DiD-labeled DENV particles by gel filtration on a Sephadex G-50 column in HNE buffer (GE Heathcare, Sweden). Labeled-DENV particles were store at 4°C.

2.5 *Fluorescence Confocal Microscopy Imaging*

Images of fluorescent samples were acquired with an Olympus FluoView 1000 confocal microscope equipped with a 60× oil immersion objective with a numerical aperture (N.A.) of 1.4. Huh7.5 cells were inoculated on a 3.5 cm glass-bottom plate (Mettek, USA). DENV-infected cells were fixed with 3.7% formaldehyde for 5 min at room temperature. After PBS washed, samples were kept in imaging buffer containing phenol red free DMEM, 75 mM HEPES, and 2% glucose and added DAPI for nucleus staining. Lysosomes were stained with 1 μM of Lysotracker (Invitrogen, USA) for 30 min. Images were captured in the green (GFP), red (Lysotracker), and far-red (DiD) channels, respectively. All images were analyzed by Olympus software FV10-ASW Viewer version 3.1. The selected confocal images were further deconvoluted by the Huygens Essential software (Scientific Volume Imaging B.V., Hilversum, The Netherlands).

2.6 *Real-Time Epi-Fluorescence and Differential Interference Contrast (DIC) Microscopy System*

The tracking experiments were conducted as described previously.[8,26,39] To capture a simultaneous image of DiD-labeled DENV particles and GFP-tagged LC3 puncta, DiD was excited with a 633 nm helium–neon laser (Melles-Griot, USA), whereas GFP was excited with a 488-nm laser (Coherent, USA). Live-cell imaging was recorded by using an inverted microscope (IX 71, Olympus, Japan) equipped with an imaging split system (U-SIP, Olympus, Japan), a high sensitivity monochrome charge-coupled devide (CCD camera (CoolSNAP HQ2, Photometrics, USA). A triple-band dichromatic mirror (Semrock, USA) was used to reflect the laser lines onto the samples. The fluorescent emission was collected by a 100× oil immersion objective with a N.A. of 1.40 (Olympus, Japan). The emission signals of the samples were first spectrally

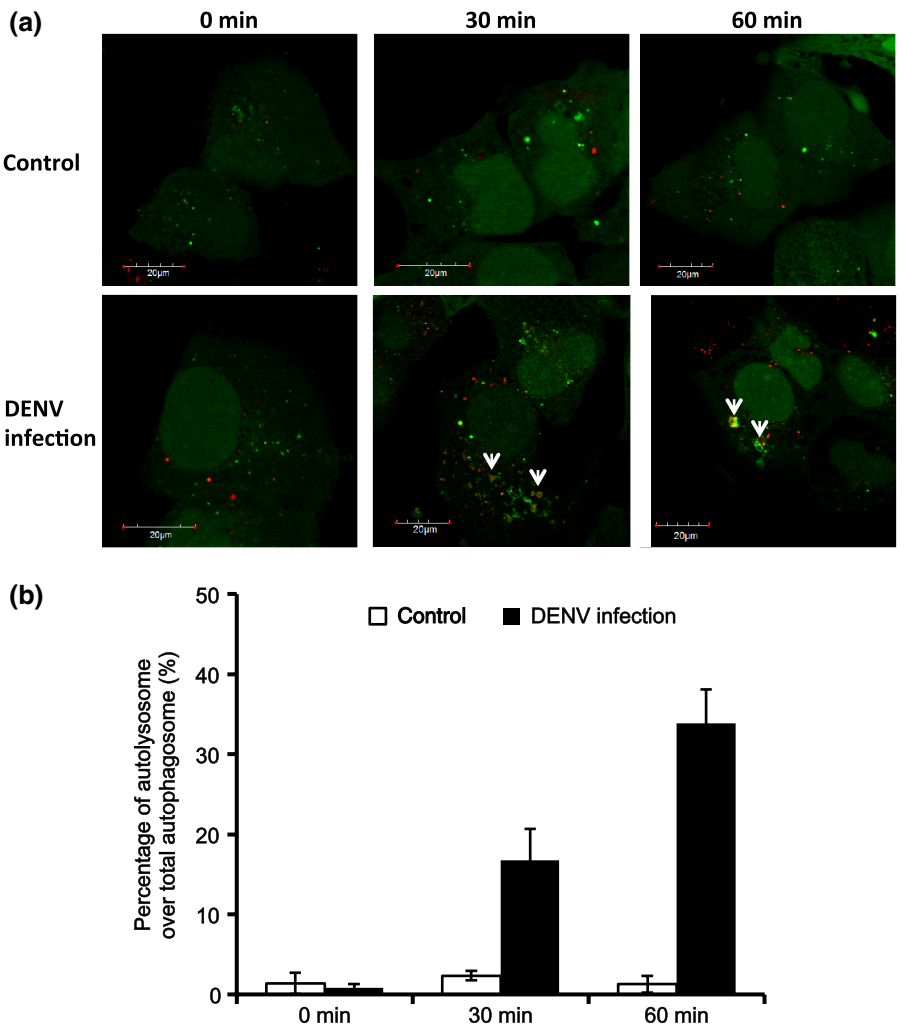

Fig. 1 Induction of autophagy by Dengue virus (DENV) in Huh7.5 cells. (a) Stably expressed GFP-LC3 Huh7.5 cells were grown on a 3.5 cm glass-bottom plate. Cells were mock-infected (top panel) or DENV-infected (bottom panel) at a multiplicity of infection (MOI) of 10 for the indicated time. Fluorescence signals were observed using an Olympus FluoView 1000 confocal microscopy. GPF-LC3 puncta was shown in green. Lysosomes were visualized by lysotracker and shown in red. White arrows indicate the location of autolysosomes. The scale bar represents 20 μm. (B) The formation of autophagolysosomes was quantified in the absence (white bar) and presence (black bar) of DENV at 0, 30, and 60-min postinfection, respectively. The percentage of the autolysome was calculated by the number of lysosomes overlapped with autophagosomes divided by the total number of autophagosomes. At least 10 cells were examined in each group. The error bars represent standard deviation.

separated by a 660 nm long-pass dichromatic mirror (Chroma Technology, USA). A 512/630-25 nm band-pass filter (Semrock, USA) was used for GFP fluorescent emission and a 665 nm long-pass filter (Chroma Technology, USA) was used for DiD emission. The separated emission signals were imaged onto the two half areas of the CCD camera. To make sure that the shapes of the cells were not significantly altered during the recording period, the nucleus and plasma membrane of the cell were identified using the differential interference contrast (DIC) optics (Olympus, Japan) before and after the fluorescence imaging. Live-cell recordings were conducted in the live cell instrument (Leica, Germany) at 37°C with 5% CO_2 supplement. Time-lapse image sequences were recorded by RS Image version 1.9.2 (Roper Scientific, Inc., USA).

2.7 *Particle Tracking*

The positioning processing of DENV particles was described previously,[40] as implemented in a MATLAB-based Polyparticletracker program. Briefly, it is comprised of five steps: First, image noise is reduced and smoothed by convolving the image with a Gaussian function: $I(x,y) = \sum_{i=-\omega}^{\omega}\sum_{j=-\omega}^{\omega} I_{\mathrm{raw}}(x+i,y+j)\exp\{-[(i^2+j^2)/4\lambda^2]\}$. Second, single particles are tracked and particle center coordinates are estimated. Third, subpixel refinement of the particle coordinates by polynomial fitting with Gaussian weight (PFGW). Next, particle discrimination and parameter are calculated. Finally, the particle positions between individual frames are connected by straight lines to form the trajectories of particles by the Polyparticletracker program.[40] Following these procedures, over 50 DENV particles in 20 cells were tracked in the present work.

3 Results

3.1 *DENV Induces Host Cellular Autophagic Responses*

In order to examine whether DENV infection triggers autophagy responses of host cells at the early steps of infection, DENV was infected into the Huh7.5 cells that stably express GFP-fused LC3 and autophagy was detected by the formation of LC3 puncta, an indicator of autophagosome. Compared to the control group [Fig. 1(a), top panel], confocal images clearly showed that DENV induced the formation of GFP-LC3 puncta at 30 and 60-min postinfection [Fig. 1(a), green dots in the bottom panel], suggesting that the formation of autophagosome could be induced by DENV during the early stage of infection. In addition, Lysotracker staining revealed that lysosomes were engulfed into LC3 puncta dramatically at 30 and 60-min postinfection, indicating the formation of autophagolysosomes, the ultimate vesicle of autophagy progression [Fig. 1(a), red dots in the bottom panel). The numbers of the autophagolysosomes were elevated by DENV infection in a time-dependent manner, compared to the DENV-free groups [Fig. 1(b)]. Taken together, these results implied that DENV infection could induce autophagy responses and form autophagolysosomes at the early step of infection.

3.2 *Visualization of DENV Particles by a Lipophilic Fluorescent Dye*

To investigate whether DENV was transported into autophagosomes during infection, a single-virus tracking experiment was conducted. Fluorescent DENV particles were first prepared by labeling with a lipohilic fluorescence dye, DiD.[28,29,39] Fluorescence-labeled viral particles were separated from excess free DiD dye by a Sephadex G-50 column. Compared to the fraction of the 40 nm fluosphere signals, the fluorescent signal of DiD appeared from fraction 5 to fraction 7 [Fig. 2(a), red

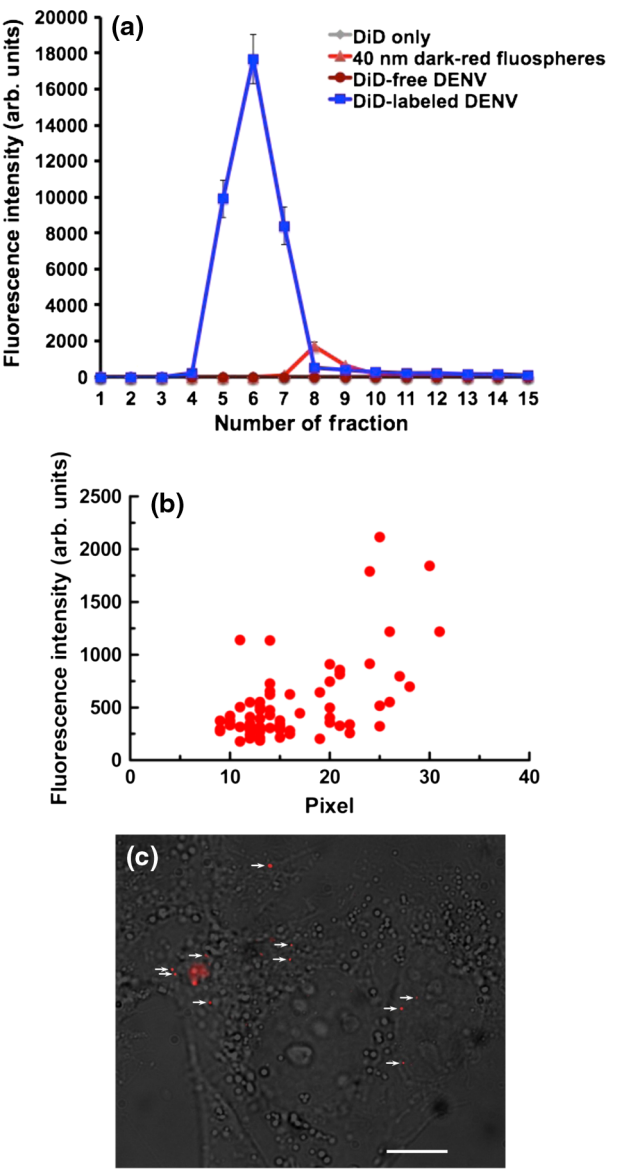

Fig. 2 Purification and characterization of DiD-labeled DENV particles. (a) DiD-labeled DENV particle was purified within the fraction layer 5 to 7 from gel filtration (blue squares). No fluorescence signal was detected neither in DiD only (gray diamonds) nor DiD-free DENV (dark red circles) within the same fraction layers. The 40 nm fluorescence microspheres were used as a size marker (red triangles). The error bars represent standard deviation. (b) The intensity and size of DiD-labeled DENV were determined by fluorescence microscopy and plotted in a graph. Particles with low fluorescence intensity (0 to 750 AU) were selected for image analysis. (c) Huh7.5 cells were infected with DiD-labeled DENV virus at a MOI of 10. The morphology of the cell was detected using differential interference contrast (DIC) optics (Olympus, Japan) after the fluorescence imaging. Fluorescence images of single DENV particles acquired by fluorescence microscopy were indicated in red (white arrow). Merge image from both DIC image and fluorescent image clearly demonstrated the DENV particle spots. The scale bar represents 10 μm.

Table 1 Effect of DiD-labeling on the infectivity of DENV. Plaque assays were performed to determine the infectivity of DENV particles incubated with DiD for indicated time periods. DiD-free DENV was used as a control. All virus particles were purified from the same fractions of the Sephadex G-50 column. The results were determined by at least three independent experiments.

DiD-labelling time	DiD-free virus	10 min	30 min	60 min
Titer (PFU/ml)	$1.08 \pm 0.53 \times 10^5$	$1.00 \pm 0.3 \times 10^5$	$1.58 \pm 0.49 \times 10^5$	$0.91 \pm 0.64 \times 10^5$

triangles and blue squares]. No fluorescence signal was detected in the same range of fractions from neither the DiD-free DENV group nor the DiD only group [Fig. 2(a), green circles and gray diamonds]. These results indicated that DENV particles were successfully labeled with DiD. The infectivity of DiD-labeled DENV was then determined by the plaque assay. Results showed that the DiD-positive fraction indeed contained infectious DENV particles (Table 1). Furthermore, compared to the label-free viruses, DiD-labeled DENV particles possessed similar infectious activities, suggesting that the DiD-labeling procedure has no significant influence on the infectivity of DENV (Table 1). To further characterize the properties of DiD-labeled DENV, DiD-labeled viral particles were added to a glass coverslip, and the size and the fluorescent intensity of DiD-labeled virus were measured. Since clusters of DENV particles formed in the preparation or the counting procedure may be considered as a single particle, the correlation between fluorescent intensity and pixel size of DiD-labeled DENV particles was evaluated. The majority of the fluorescent bright dots had relatively smaller sizes (10 to 20 pixels) and lower fluorescence intensity [250 to 750 arbitrary units (AU)], presumably indicating these DiD-labeled viral particles possess a similar brightness, and most probably represent a single DENV particle [Fig. 2(b)]. However, there were approximately one-fourth of fluorescent particles that exhibited stronger fluorescence and larger pixel sizes, indicating that they might be aggregated viral particles. The combination of the fluorescent image of single DENV particles with the DIC image of Huh7 cells revealed that DiD-labeled DENV particles possess a good signal-to-noise (S/N) ratio allowing single viral particles to be clearly detected [Fig. 2(c)].

3.3 *DENV Particles Co-Localized with LC3 Puncta During Virus Infection*

To confirm the localization of DENV particles during the early stage of infection, GFP-LC3 stably expressed Huh-7.5 cells were infected with DiD-labeled DENV particles at MOI of 10. At the initial time point, confocal microscopy images showed that DiD-labeled DENV particles surrounded Huh7.5 cells, indicating the attachment of DENV particles on the cellular surface of Huh7.5 cells [Fig. 3(a)]. In addition, only a few GFP-LC3 puncta were observed at this time point. Consistent with the previous results in Fig. 1, the number of GFP-LC puncta was dramatically increased by DENV infection from 15 to 60 min [Fig. 3(a)]. DiD-labeled DENC particles were found to co-localize with GFP-LC3 puncta at 15 min after internalization. Quantitative analyses further showed that the number of DENV particles co-localized with autophagosome significantly increased with the infectious time ($p < 0.0001$) [Fig. 3(b)], suggesting that DENV particles entered into autophagosome during the early stage of infection. Furthermore, three-dimensional (3-D) images from confocal Z-stack images revealed that DENV particles co-localized with LC3 puncta and were surrounded by GFP-LC3 [Fig. 3(c)]. Cross sectional analyses using fluorescence intensity profiling displayed the signal distribution of GFP-LC3 and DiD-labeled virus particles, suggesting that DENVI-induced autophagosomes indeed engulfed DENV particles [Fig. 3(c)]. These results demonstrated that DENV particles were translocated into autophagosomes within 15-min postinfection.

3.4 *Trajectory Analysis of Single DENV Particle and GFP-LC3 Puncta Interaction*

Time-lapse dual-channel fluorescence microscopy images allowed us to perform single-virus tracking in living cells.[26] The setup of a home-built real-time dual-fluorescence microscopy was shown in Fig. 4(a) and described in detail in Sec. 2. To examine the mechanical stability and to exclude surrounding vibration, we calculated the standard deviations of positions by the time-lapsed imaging of an immobile specimen. Fluorescent microspheres with a 200-nm diameter were spread onto glass coverslips and fixed by a mounting medium, and the fluorescence images were captured for 5 min at a frame rate of 2 frames/ min. The central fluorescence intensity distribution [Fig. 4(b), gray line] of the fluorescent microsphere spots [Fig. 4(b), upper right] were examined by ImageJ software and fitted by Gaussian function [Fig. 4(b), red line]. The standard deviation of the diameter of an identified spot was 0.21 pixels or 13.95 nm in real scale. The relative error was smaller than 2.8%, suggesting that the microscope system would be stable for single-virus tracking. Prior to tracking single viral particles in live cells, we also determined the tracking accuracy of DiD-labeled DENV particles by examining the central fluorescence intensity distribution [Fig. 4(c), gray line] of viral spots [Fig. 2(d), upper right] fitted by Gaussian function [Fig. 2(d), green line]. The tracking accuracy (σ) was calculated as follows:, where s is the standard deviation of the point spread function in pixels, and S/b is the S/N ratio. According to the measurement of 30 individual viral particles, the tracking accuracy was determined at 0.078 pixels, or 4.98 nm in real scale. The relative error was smaller than 0.4%, indicating that DiD-labeling provided an SN ratio high enough for estimating particle positions. In order to visualize the movement of a single DENV particle in a live cell, cells were infected with DiD-labeled DENV in the presence or absence of chlorpromazine (CPZ), a cationic amphiphilic drug that inhibited the formation of clathrin-coated pits to block clathrin-mediated cytocytosis. Compared to the CPZ-free group, the treatment of CPZ displayed significant effects to restrict trajectories of DENV particles [Fig. 4(d), left panel]. Furthermore, we plotted the mean-square displacement (MSD) of each viral particle of CPZ treatment [Fig. 4(d), right panel]. Simple diffusion should

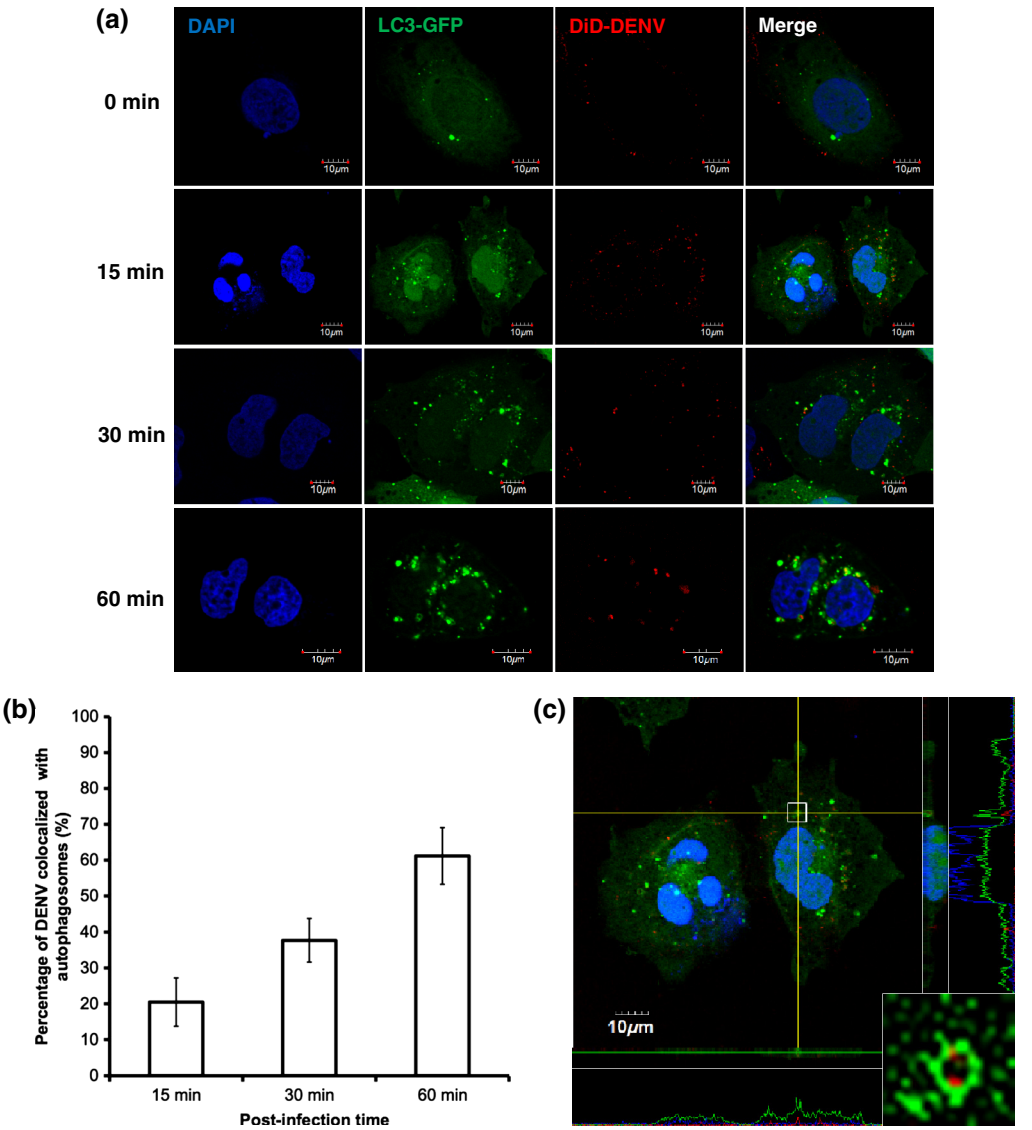

Fig. 3 Co-localization of DENV particles and autophagosomes. (a) Huh7.5 cells were infected with DiD-labeled DENV at an MOI of 10 for the indicated time. Fluorescence images were acquired using an Olympus FluoView 1000 confocal microscopy. GPF-LC3 puncta was shown in green. Nuclei were visualized by DAPI staining. The scale bar represents 10 μm. (b) Quantification of co-localized DiD-labeled DENV particles with GFP-LC3 puncta. Percentage of co-localization was determined by the number of viral particles with GFP-LC3 puncta divided by total DENV particles. A statistical analysis was undertaken by one-way analysis of variance using SPSS with $p < 0.0001$ for significance. The numbers of the examined cells at each time point were 28, 26, and 22. (c) The three-dimensional reconstruction of the Z-stacked deconvolved image showed the engulfed DENV particles by autophagosomes. In fluorescence intensity profiling, the signal distribution of GFP-LC3 and DiD-labeled virus particles was indicated in green and red, respectively.

display a linear relationship between MSD and time, and an upward curvature would indicate a directed motion.[8] In the absence of CPZ, an upward curvature suggested that DENV particles were transported within the cells [Fig. 4(d), top right panel]. In contrast, a linear mode of MSD in the presence of CPZ indicated that DENV moved on the cell surface in a simple diffusion manner [Fig. 4(d), right bottom panel], suggesting that DENV particles were unable to enter cells but were attached on the cell surface.

Subsequently, we would like to investigate whether DENV particles interact with autophagosomes. If the interaction of DENV particle with autophagosomes was one of the early events after viral entrance, the intracellular trajectories of both should be overlapped during viral infection. The fluorescent signals of DiD-DENV particles and GFP-LC3 puncta were simultaneously recorded by a time-lapsed fluorescence microscopy. After 30-min incubation at 4°C for DENV attachment, Huh7.5 cells were placed on the object table in the culture chamber of time-lapsed fluorescence microscopy at 37°C and two-color fluorescence series images were recorded. In Fig. 5(a), the DiD-DENV particles were shown in red, GFP-LC3 puncta in green, and the vesicles containing both DiD-DENV and GFP-LC3 puncta in yellow. Clearly, these images revealed the co-localization of DENV and LC3 puncta [Fig. 5(a)]. The trajectories of both DiD-DENV and GFP-LC3 puncta were also shown to be almost identical [Fig. 5(b)], strongly suggesting that DENV particles traveled with LC-3 pancta. Therefore, we concluded that DENV particles interacted with autophagosomes during the early stage of viral infection.

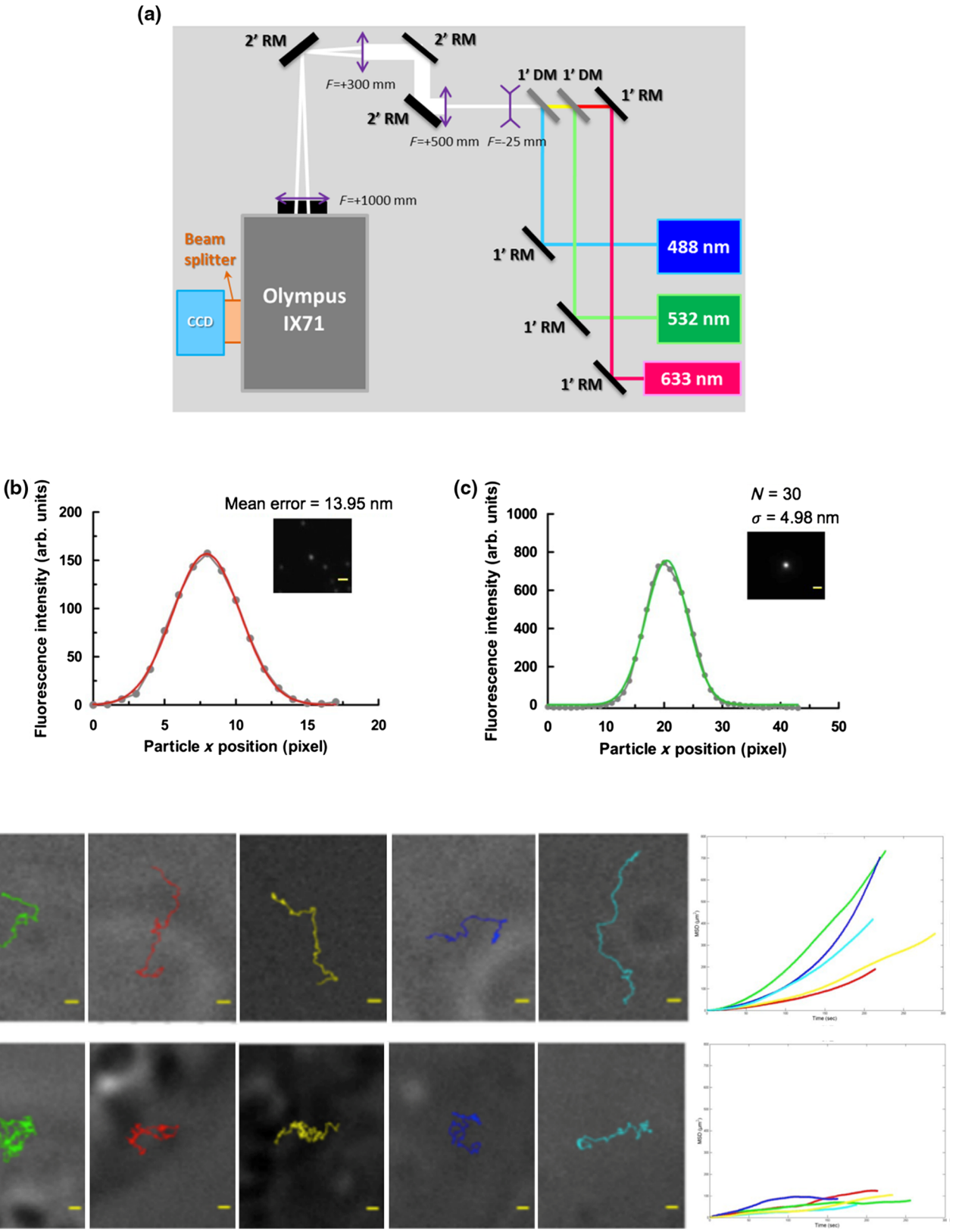

Fig. 4 Single-virus particle tracking by real-time epi-fluorescence microscopy. (a) Schematic diagram of the setup of the microscopy system. (b) Represented the central one-dimension (1-D) fluorescence intensity distribution of 200 nm fluorescence microspheres spot (gray line) and Gaussian fitting (red line). The upper right image was shown a single fluorescence microsphere spot. The scale bar represents 1 μm. (c) Represented the central 1-D fluorescence intensity distribution of DiD-labeled DENV-2 particle spot (gray line) and Gaussian fitting (green line). The upper right image showed a single DiD-labeled DENV particle spot and the scale bar represents 1 μm. (d) The two-dimensional trajectories of DENV within Huh7.5 cells in the absence (top panel) or presence (bottom panel) of CPZ, an inhibitor of clathrin-mediated cytocytosis were shown. Both motion trajectories (right panel) and MSD analysis (left panel) graph showed corresponding colors for individual DiD-labeled DENV particles. The scale bars represent 1 μm.

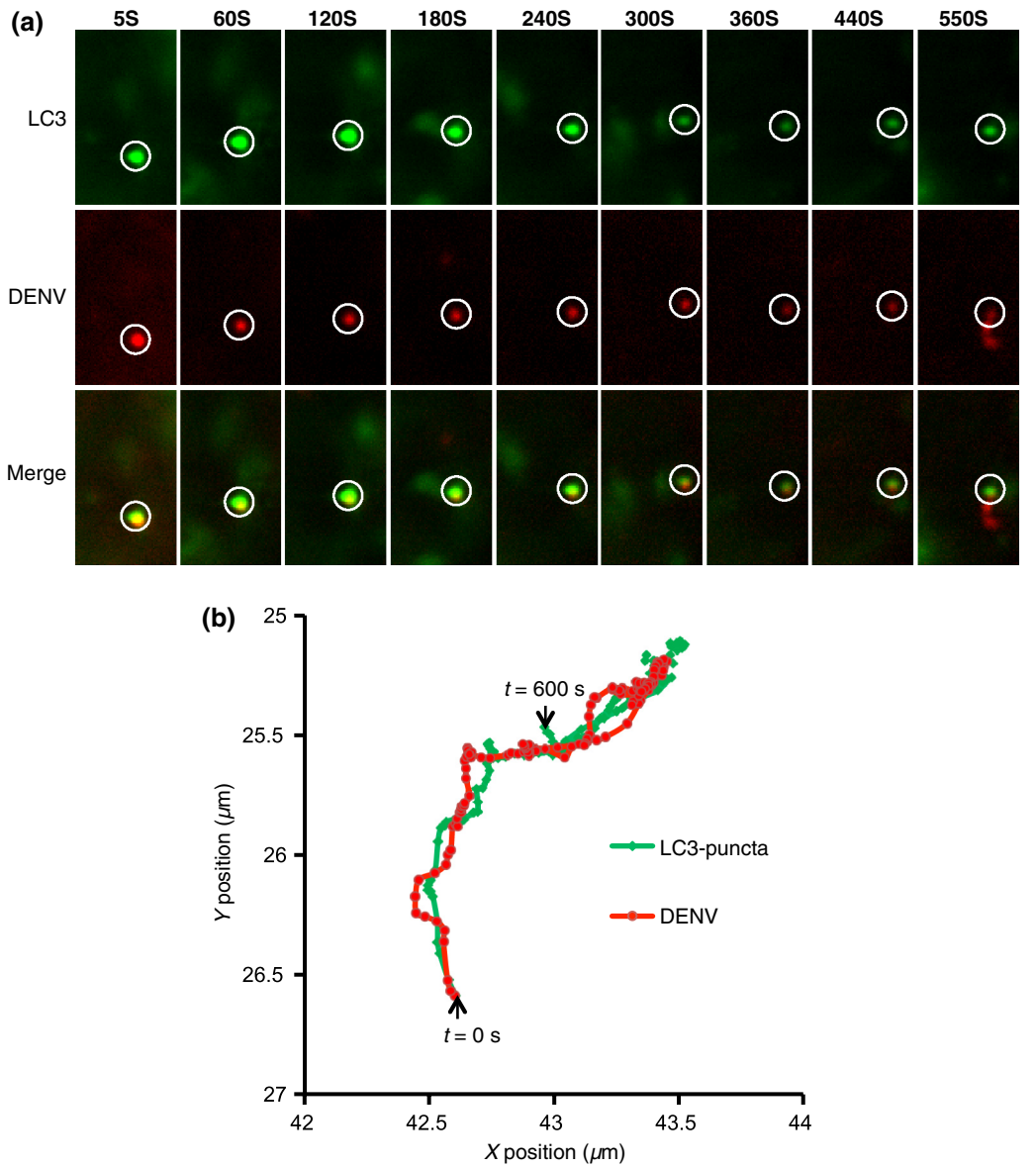

Fig. 5 Co-transportation of DENV particles and autophagosomes. (a) The selected frames showed the endocytic trafficking behavior of a single DiD-labeled DENV particle co-localized with GFP-LC3 luncta. The GFP-LC3 puncta were displayed in green (top panel), the DiD-labeled DENV particles in red (middle panel), and the vesicles containing both DiD-DENV and GFP-LC3 puncta in yellow (bottom panel). (b) The overlapped trajectory profiles of DENV particle (in red) and LC3 puncta (in green) in Huh7.5 cell were determined by Polyparticletracker (Ref. 40). Black arrow indicates the start point of tracking.

3.5 *Inhibition of Autophagy Changes DENV Distribution in Host Cells*

Previous studies have shown that DENV induces autophagy in various types of cells.[21,22,24,25,41] In the present work, DENV infection was able to induce autophagic responses and caused the formation of autophagosomes that engulfed the DENV particles (Figs. 1 and 3). It was intriguing to investigate the influence of DENV-induced autophagy on the production of the virus. Extracellular virus titers from the culture supernatant of the infected cells in the presence of the autophagy suppressor 3-MA and the autophagy stimulator rapamycin, respectively, were determined by the plaque assay. Virus yield was reduced in 3-MA treated cells and increased in response to the rapamycin treatment [Fig. 6(a)]. Moreover, it would be interesting to examine whether the intracellular location of DENV particles was altered while Huh-7.5 cells were treated with either 3-MA or rapamycin. At the initial step of infection, DENV-induced formation of autophagosomes was suppressed dramatically by the treatment of 3-MA [Fig. 6(b)]. In addition, compared to the distribution of DENV particles in drug-free cells [Fig. 3(a)], the internalized virus particles were dispersed in the cytoplasm of 3-MA treated cells instead of in the perinuclear region 30-min postinfection [Fig. 6(b)]. These results revealed that the treatment of 3-MA not only suppressed autophagosome formation but also altered the distribution of DENV particles in the host cells. On the other hand, autophagosomes were stimulated dramatically in rapamycin-treated Huh7.5 cells 30 min after DENV infection [Fig. 6(c)]. As expected, DENV particles were engulfed by autophagosomes and distributed in the

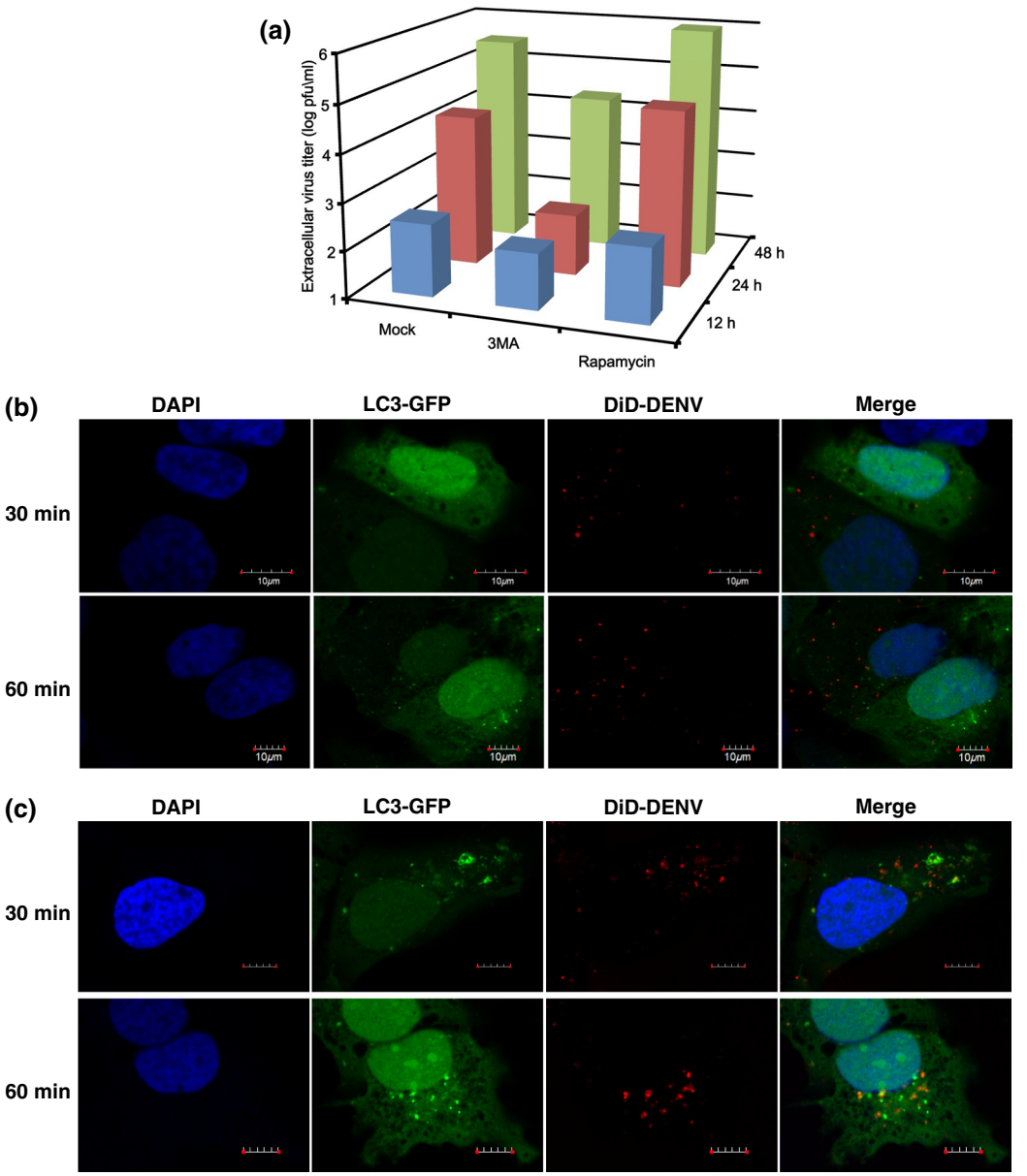

Fig. 6 The effects of 3-methyladenine (3-MA) and rapamycin on the production of DENV and the distribution of DENV particles. Huh7.5 cells treated with either the autophagy suppress 3-MA or the autophagy stimulator rapamycin, respectively, were infected with DiD-labeled DENV at an MOI of 10 for the indicated time. (a) The amounts of newly produced virus isolated from the culture supernatant of the infected cells were determined by plaque assay at 12, 24, and 48-h postinfection. The data were derived from three independent replicates. (b and c) Using an Olympus FluoView 1000 confocal microscopy, fluorescence images of DENV particle (in red) and autophagosomes (in green) were acquired at 30 and 60 min in the presence of 3-MA (b) or rapamycin (c). GPF-LC3 puncta was shown in green. Nuclei were visualized by DAPI staining. The scale bar represents 10 μm.

perinuclear region of cytoplasm [Fig. 6(c)]. In summary, the location of DENV particles is affected due to the alteration of autophagy status, resulting in the alteration of DENV replication.

4 Discussion

In this study, we have uncovered a novel early event of DENV infection. First, DENV can induce Huh-7.5 cell autophagic responses and trigger the formation of autophagosomes within 30-min postinfection. Z-stacking 3-D image analyses revealed that autophagosomes engulfed DENV particles. In addition, using single-virus particle tracking, the trafficking dynamics of autophagosomes and internalized DENV particles showed near-identical intracellular trajectories, strongly suggesting that DENV particles interacted directly with autophagosomes. Finally, the intracellular distribution of DENV particles was altered in the presence of the pharmacological drugs to either suppress or stimulate autophagic responses in DENV-infected cells during the first 30 min of infection, implying that virus-induced autophagosomes can facilitate the delivery of DENV particles from the entry site to the replication site. Taken together, this study not only provides new insights regarding the interactions between DENV and cellular autophagic responses, but also offers a better opportunity for using photonics tools to investigate virus–host interactions.

Growing evidence indicates that autophagy is required for the RNA genome replication of DENV and autophagosomes may be the putative location of viral replication.[21–25] On

contrary, using cryo-EM tomography, Welschet al. recently showed that the 3-D structure of DENV replication complexes was associated with the ER membrane instead.[12] In this study, we used DiD-labeled single-virus particle tracking to clearly demonstrate that DENV particles were translocated into autophagosomes through a clathrin-mediated endocytosis within 30-min postinfection [Figs. 3 and 4(d)]. These results strongly supported that DENV particles indeed interact with autophagosomes. It will be worthy to further investigate which components of autophagosomes interact with DENV particles in the future.

After clathrin-mediated endocytosis, the itinerary of DENV particles has been shown from early endosome to late endosome prior to fusion within the acidic endosomes.[7,8,39] In addition, DENV replication complexes are proposed to be in either ER cisternae or autophagosomes.[12,22,25] These results raise an important issue regarding how RNA genome is delivered to the replication site. At least two possible mechanisms may address this question. First, DENV particle-containing vesicles are directly targeted by autophagy and DENV particles undergo the uncoating process within autophagolysomes, in which DENV RNA genome might be translocated into autophagolysosomes for genome replication.[22] The other possibility might be that RNA genome released from acidic late endosomes after the uncoating process of DENV particles is delivered to the replication site through an unidentified mechanism.[8,9] According to the confocal images and real-time single DENV particle tracking, DiD-labeled DENV particles are internalized through clathrin-mediated endocytosis and transported into autophagosomes [Figs. 3, 4(d), and 5], supporting the first hypothesis. Furthermore, DENV spread in cytoplasm but not in the perinuclear region after 30-min postinfection in the presence of 3-MA [Fig. 6(b)]. This was consistent with the distribution of DENV particles in 15-min postinfection [Fig. 3(a)], suggesting that intracellular trafficking of DENV particles could be blocked by 3-MA to prevent the translocation of DENV to autophagosomes, resulting in the inhibition of the viral production [Fig. 6(a)]. In addition, some RNA viruses can subvert autophagy pathway to facilitate their replication.[19,42,43] Based on the current results and previous studies,[22,25,43] therefore, we would like to propose that DENV particles are first transported into endosomes and converted into autophagosome, which eventually facilitates the production of the virus. Further studies are needed in order to address the following issues: whether the DENV RNA genome is released into the autophagosome, whether the viral replication site is located in autophagosomes, and whether virus-loaded endosomes are directly fused with the existing autophagosomes or are engulfed by newly formed autophagosomes.

Previous studies showed that GFP-LC3 puncta do not co-localize with DENV replication markers by using the immunofluorescence staining assay.[21] It is probably due to immunoreagents that cause the re-localization of target molecules and do not reflect the *in vivo* situation.[44] In addition, most observations showing the co-location of DENV and autophagosomes were done at least 24-h postinfection.[22,25,41] There is so far no evidence elucidating the interaction of DENV particles with autophagosomes within 1-h postinfection because of limited sensitivity in detecting small amounts of viral proteins and the RNA genome at the early stage of infection. Recent developments of single-virus particle detection provide an approach with a high SN ratio for the visualization of various types of viruses.[27,28,38] Using the single-virus particle tracking approach, we successfully elucidated for the first time that DENV particles were located in autophagosomes and traveled together during the early stage of infection [Figs. 3(c) and 5].

For the past decade, fluorescence microscopy has demonstrated its capacity to achieve a single-molecule localization accuracy within a few nanometers, well below the resolution limit of conventional microscopy.[45] Single-virus tracking combined with the single-molecule localization and real-time imaging is a new approach to monitor individual virus particles or viral components in living cells.[26] This modern technique could provide a novel view that impacts traditional biology. In this study, the combination of modern microscopy techniques, cell biology, and pharmacology has successfully proven that autophagosomes participate in DENV cellular trafficking during the early infectious stage, which would be of great value in the development of antiviral drugs.

Acknowledgments

We are thankful to Dr. Michael M.C. Lai for kindly providing reagents and Dr. Arthur Chiou for the assistance of the imaging system setup. The authors also thank Dr. Chuang-Rung Chang and Dr. Janice Fon for their critically reading and editing this article. This work was supported by grants from the Ministry of Education, Aim for the Top University Plan (100AC-T406, 101AC-T406) to Y.-H.P., Veterans General Hospitals and University System of Taiwan Joint Research Program (VGHUST 102-G6-2-4), Taipei City Hospital (TCH 95002-62-079) to Y.-H.P., and the National Science Council, Taiwan (NSC 95-3112-B-010-013, NSC 96-3112-B-010-006, NSC 97-3112-B-010-004, and NSC 102-2320-B-010-018) to Y.-H.P., (NSC 100-2112-M-001-022-MY3) to C.-H.L.

References

1. J. S. Mackenzie, D. J. Gubler, and L. R. Petersen, "Emerging flaviviruses: the spread and resurgence of Japanese encephalitis, West Nile and dengue viruses," *Nat. Med.* **10**(12 Suppl.), S98–S109 (2004).
2. C. P. Simmons et al., "Dengue," *N. Eng. J. Med.* **366**(15), 1423–1432 (2012).
3. D. J. Gubler and G. G. Clark, "Dengue/dengue hemorrhagic fever: the emergence of a global health problem," *Emerg. Infect. Dis.* **1**(2), 55–57 (1995).
4. J. G. Rigau-Perez et al., "Dengue and dengue haemorrhagic fever," *Lancet* **352**(9132), 971–977 (1998).
5. H. Y. Lei et al., "Immunopathogenesis of dengue virus infection," *J. Biomed. Sci.* **8**(5), 377–388 (2001).
6. Y. Modis et al., "Structure of the dengue virus envelope protein after membrane fusion," *Nature* **427**(6972), 313–319 (2004).
7. M. N. Krishnan et al., "Rab 5 is required for the cellular entry of dengue and West Nile viruses," *J. Virol.* **81**(9), 4881–4885 (2007).
8. H. M. van der Schaar et al., "Dissecting the cell entry pathway of dengue virus by single-particle tracking in living cells," *PLoS Pathog.* **4**(12), e1000244 (2008).
9. E. Zaitseva et al., "Dengue virus ensures its fusion in late endosomes using compartment-specific lipids," *PLoS Pathog.* **6**(10), e1001131 (2010).
10. N. Shrivastava et al., "Insights into the internalization and retrograde trafficking of Dengue 2 virus in BHK-21 cells," *PLoS One* **6**(10), e25229 (2011).
11. L. L. Li et al., "Positive transcription elongation factor b (P-TEFb) contributes to dengue virus-stimulated induction of interleukin-8 (IL-8)," *Cell. Microbiol.* **12**(11), 1589–1603 (2010).
12. S. Welsch et al., "Composition and three-dimensional architecture of the dengue virus replication and assembly sites," *Cell Host Microbe* **5**(4), 365–375 (2009).

13. D. J. Klionsky, "Autophagy: from phenomenology to molecular understanding in less than a decade," *Nat. Rev. Mol. Cell Biol.* **8**(11), 931–937 (2007).
14. H. Weidberg, E. Shvets, and Z. Elazar, "Biogenesis and cargo selectivity of autophagosomes," *Annu. Rev. Biochem.* **80**, 125–156 (2011).
15. N. Mizushima et al., "Autophagy fights disease through cellular self-digestion," *Nature* **451**(7182), 1069–1075 (2008).
16. B. Levine and G. Kroemer, "Autophagy in the pathogenesis of disease," *Cell* **132**(1), 27–42 (2008).
17. A. I. Chiramel, N. R. Brady, and R. Bartenschlager, "Divergent roles of autophagy in virus infection," *Cells* **2**(1), 83–104 (2013).
18. T. X. Jordan and G. Randall, "Manipulation or capitulation: virus interactions with autophagy," *Microbes Infect.* **14**(2), 126–139 (2012).
19. K. Kirkegaard, "Subversion of the cellular autophagy pathway by viruses," *Curr. Top. Microbiol. Immunol.* **335**, 323–333 (2009).
20. N. S. Heaton and G. Randall, "Dengue virus and autophagy," *Viruses* **3**(8), 1332–1341 (2011).
21. N. S. Heaton and G. Randall, "Dengue virus-induced autophagy regulates lipid metabolism," *Cell Host Microbe* **8**(5), 422–432 (2010).
22. M. Panyasrivanit et al., "Co-localization of constituents of the dengue virus translation and replication machinery with amphisomes," *J. Gen. Virol.* **90**(2), 448–456 (2009).
23. M. Panyasrivanit et al., "Linking dengue virus entry and translation/replication through amphisomes," *Autophagy* **5**(3), 434–435 (2009).
24. A. Khakpoor et al., "A role for autophagolysosomes in dengue virus 3 production in HepG2 cells," *J. Gen. Virol.* **90**(5), 1093–1103 (2009).
25. Y. R. Lee et al., "Autophagic machinery activated by dengue virus enhances virus replication," *Virology* **374**(2), 240–248 (2008).
26. B. Brandenburg and X. Zhuang, "Virus trafficking—learning from single-virus tracking," *Nat. Rev. Microbiol.* **5**(3), 197–208 (2007).
27. B. Brandenburg et al., "Imaging poliovirus entry in live cells," *PLoS Biol.* **5**(7), e183 (2007).
28. M. Lakadamyali et al., "Visualizing infection of individual influenza viruses," *Proc. Natl. Acad. Sci. U. S. A.* **100**(16), 9280–9285 (2003).
29. M. Lakadamyali, M. J. Rust, and X. Zhuang, "Ligands for clathrin-mediated endocytosis are differentially sorted into distinct populations of early endosomes," *Cell* **124**(5), 997–1009 (2006).
30. M. J. Rust et al., "Assembly of endocytic machinery around individual influenza viruses during viral entry," *Nat. Struct. Mol. Biol.* **11**(6), 567–573 (2004).
31. G. Seisenberger et al., "Real-time single-molecule imaging of the infection pathway of an adeno-associated virus," *Science* **294**(5548), 1929–1932 (2001).
32. K. E. Coller et al., "RNA interference and single particle tracking analysis of hepatitis C virus endocytosis," *PLoS Pathog.* **5**(12), e1000702 (2009).
33. K. Miyauchi et al., "HIV enters cells via endocytosis and dynamin-dependent fusion with endosomes," *Cell* **137**(3), 433–444 (2009).
34. D. McDonald et al., "Visualization of the intracellular behavior of HIV in living cells," *J. Cell Biol.* **159**(3), 441–452 (2002).
35. H. P. Babcock, C. Chen, and X. Zhuang, "Using single-particle tracking to study nuclear trafficking of viral genes," *Biophys. J.* **87**(4), 2749–2758 (2004).
36. S. Kimura, T. Noda, and T. Yoshimori, "Dissection of the autophagosome maturation process by a novel reporter protein, tandem fluorescent-tagged LC3," *Autophagy* **3**(5), 452–460 (2007).
37. W. C. Su et al., "Rab5 and class III phosphoinositide 3-kinase Vps34 are involved in hepatitis C virus NS4B-induced autophagy," *J. Virol.* **85**(20), 10561–10571 (2011).
38. N. V. Ayala-Nunez, J. Wilschut, and J. M. Smit, "Monitoring virus entry into living cells using DiD-labeled dengue virus particles," *Methods* **55**(2), 137–143 (2011).
39. H. M. van der Schaar et al., "Characterization of the early events in dengue virus cell entry by biochemical assays and single-virus tracking," *J. Virol.* **81**(21), 12019–12028 (2007).
40. S. S. Rogers et al., "Precise particle tracking against a complicated background: polynomial fitting with Gaussian weight," *Phys. Biol.* **4**(3), 220–227 (2007).
41. M. Panyasrivanit et al., "Induced autophagy reduces virus output in dengue infected monocytic cells," *Virology* **418**(1), 74–84 (2011).
42. R. Mateo et al., "Inhibition of cellular autophagy deranges dengue virion maturation," *J. Virol.* **87**(3), 1312–1321 (2013).
43. W. T. Jackson et al., "Subversion of cellular autophagosomal machinery by RNA viruses," *PLoS Biol.* **3**(5), e156 (2005).
44. U. Schnell et al., "Immunolabeling artifacts and the need for live-cell imaging," *Nat. Methods* **9**(2), 152–158 (2012).
45. S. Herbert et al., "Single-molecule localization super-resolution microscopy: deeper and faster," *Microsc. Microanal.* **18**(6), 1419–1429 (2012).